Modeling Separation and Reattachment Using the Turbulent Potential Model

Blair Perot & Hudong Wang

Department of Mechanical Engineering
University of Massachusetts, Amherst, MA 01003

ABSTRACT

A new type of turbulence model has recently been proposed which involves transport equations for the scalar and vector potentials of the turbulent body force (the divergence of the Reynolds stress tensor). Theoretical analysis of this turbulent potential model suggests that the predictive accuracy of Reynolds stress transport equation models might be obtained at a cost comparable to state-of-the-art two-equation turbulence models. Initial tests of the model showed promising results for simple turbulent flows such as channel flow at various Reynolds numbers, boundary layers, mixing layers, rotating channel flow, and even transition. In order to understand the model's behavior in more complex flow situations it is now tested on a number of more complex flows involving flow separation, reattachment and stagnation. Model predictions for two adverse pressure-gradient boundary layers are presented, one mild and one on the verge of separation. In addition, predictions for the backward facing step and a turbulent impinging jet are presented.

1. INTRODUCTION

Reynolds Averaged Navier-Stokes (RANS) turbulence models are usually concerned with modeling the Reynolds stress tensor. An alternative approach to RANS turbulence modeling has been proposed[1,2] where the primary modeled quantities are the scalar and vector potentials of the turbulent body force - the divergence of the Reynolds stress tensor. This approach has been found to have a number of attractive properties, most important of which is the ability to model non-equilibrium turbulence situations accurately at a cost and complexity comparable to the widely used two-equation models such as k-ε.

Like Reynolds stress transport equation models, the proposed model does not require a hypothesized constitutive relation between the turbulence and the mean flow variables. This allows non-equilibrium turbulence to modeled effectively. However, unlike Reynolds stress transport equation models, the proposed system of partial differential equations is much simpler to model and compute. It involves roughly half the number of variables, no realizability conditions, and removes the strong coupling between the equations. A analysis of the turbulent body force potentials and their physical significance[1] has revealed that they represent the relevant information contained in the Reynolds stress tensor and are fundamental turbulence quantities in their own right.

Many existing RANS models require a constitutive algebraic relation between the Reynolds stress tensor and the mean flow gradients. The most common relation is the eddy viscosity model, $\mathbf{R} = \frac{2}{3}k\mathbf{I} - \nu_T(\nabla\mathbf{u} + \nabla\mathbf{u}^T)$, where k is the turbulent kinetic energy and ν_T is the eddy viscosity. More complex constitutive relations are certainly possible[3-5] and these nonlinear eddy viscosity relations fix a number of deficiencies of the standard linear model, but they still assume that the turbulence is close to equilibrium and has had time to adjust to any changes in the mean flow. Unfortunately, many turbulent flows of practical engineering significance are not close to equilibrium. A classic example is the adverse pressure gradient boundary layer. Other examples include rapidly strained flows and three-dimensional boundary layers. The equilibrium assumption imbedded in any constitutive relation for the Reynolds stress tensor is emphasized here because the proposed model avoids such a relation and therefore has the potential to predict non-equilibrium turbulent flows more accurately.

There is some prior evidence that models which avoid a constitutive relation for the Reynolds stress tensor outperform other models of the same general class. Both examples of this phenomenon come from models developed for nearly parallel shear flows (where the Reynolds shear stress is the important Reynolds stress). For example, the zero-equation model of Johnson & King[6] solves an ordinary differential equation for the maximum turbulent shear stress. As a result it often performs better than other zero-equation models which use the traditional approach of defining an eddy viscosity. A similar result is also obtained with one and two-equation models. The model of Bradshaw, Ferriss & Atwell[7] was widely accepted to be the most accurate model of the 1968 Stanford competition[8]. This model differed from the competitors in that it solved an equation for the shear stress directly, rather than using a constitutive equation involving the mean shear. The principal drawback of both these methods (and probably the reason that they are not more popular) is that they can only be applied to nearly parallel shear flows. In some sense, the proposed model can be viewed as a way to generalize the model of Bradshaw *et. al.* to arbitrary flows.

In the past, for arbitrary flows the only alternative to using a constitutive relation was to solve modeled transport equations for the Reynolds stress tensor itself. Reynolds stress transport models can potentially contain more physics than eddy-viscosity based models, however the equations are significantly more difficult to solve. In three-dimensions one must solve six highly coupled transport equations for each Reynolds stress. The equations are stiff, and none of the Reynolds stresses are universally dominant, so uncoupling the equations numerically is very difficult. In addition, the Reynolds stress tensor is a positive definite tensor but the modeled equations often do not preserve this property (realizability[9]). The proposed model does not suffer from these difficulties. It involves half the equations of a Reynolds stress transport model. The equations are not strongly coupled and are not numerically stiff.

The key to developing a model which avoids the use of a constitutive relation and yet does not involve the complexity of a full Reynolds stress transport closure is to note that the Reynolds stresses contain more information than required by the mean flow. Only the divergence of the Reynolds stress tensor (a body force vector) is required to solve for the mean flow. With this in mind, the potential turbulence model defines two new turbulent quantities – the scalar and vector potentials of the body force vector. The advantages of a model that uses these turbulent potentials, rather than the body force vector itself, are twofold.

Firstly, this allows the momentum equation to remain a conservative equation. Secondly, and more importantly, these potentials have a very clear physical interpretation which will facilitate the construction of models for their evolution. Turbulence modeling based on the force vector itself (or its rotational component – the Lamb vector) have been proposed by Wu, Zhou & Wu[10], and Marmanis[11], but the author is not aware of any model results based on these ideas.

2. TURBULENT POTENTIALS

The scalar potential, ϕ, and vector potential, $\boldsymbol{\psi}$, of the turbulent body force are defined mathematically by the following equations.

$$\nabla\phi + \nabla\times\boldsymbol{\psi} = \nabla\cdot\mathbf{R} \tag{1a}$$

$$\nabla\cdot\boldsymbol{\psi} = 0 \tag{1b}$$

The second equation is a constraint on the vector potential. Other constraints are possible but this is the simplest for the purposes of our analysis. These equations can be rewritten to express the turbulent potentials individually.

$$\nabla^2\phi = \nabla\cdot(\nabla\cdot\mathbf{R}) \tag{2a}$$

$$\nabla^2\boldsymbol{\psi} = -\nabla\times(\nabla\cdot\mathbf{R}) \tag{2b}$$

The boundary conditions on these elliptic equations are constructed intuitively. Both potentials are required to go to zero at infinity, at a wall, or at a free surface. Note that by its very definition (Eqn. 1a) the scalar potential is the part of the turbulence that contributes to the mean pressure but does not effect the mean vorticity. Only the vector potential has the ability to effect the mean vorticity, and it only moves the vorticity around (enhanced transport), it does not create or destroy mean vorticity. Physically, we sometimes find it useful to regard the scalar potential as a measure of the average pressure drop in the cores of turbulent vortices, and the vector potential as a measure of the average vorticity magnitude of the turbulent vortices.

In flows with a single inhomogeneous direction (say the y-direction), Eqns. (2a) and (2b) simplify to $\phi = R_{22}$, $\psi_1 = -R_{23}, \psi_2 = 0, \psi_3 = R_{12}$. For this reason, it is also reasonable to view the vector potential as a conceptual generalization of the shear stress ($\overline{u'v'}$) to arbitrary geometries and three dimensions. In two-dimensional mean flows the vector potential is aligned perpendicular to the flow (like the vorticity) and has only a single nonzero component (ψ_3). The scalar potential (in combination with the turbulent kinetic energy) gives a good indication of the anisotropy of the turbulence and is fundamental to modeling the presence of walls and/or surfaces without using wall functions. The scalar potential is a positive semi-definite quantity in flows with a single inhomogeneous direction. It is hypothesized that this is also true for arbitrary flows.

In three-dimensional flows the presence of the divergence free constraint on the vector potential implies that the vector potential can be computed at a cost roughly equivalent to the scalar potential. Since the k and ε transport equations are also solved with the model, the overall complexity and cost of solving the potential model is four transport equations. This is roughly half that of a full Reynolds stress transport equation closure (seven equations), with little, if any, loss in the overall predictive capacity.

3. TURBULENT POTENTIAL MODEL

The transport equations that constitute the turbulent potential model are summarized below.

$$\frac{Dk}{Dt} = \nabla \cdot (\nu + \nu_T / \sigma_k)\nabla k + P - \varepsilon$$

$$\frac{D\varepsilon}{Dt} = \nabla \cdot (\nu + \nu_T / \sigma_\varepsilon)\nabla \varepsilon + \beta \frac{\varepsilon}{k}(C_{\varepsilon 1} P - C_{\varepsilon 2}\varepsilon) + C_{\varepsilon 3}(1-\alpha)2\varepsilon \nabla \cdot \tfrac{\phi}{\varepsilon}\nabla k$$

$$\frac{D\phi}{Dt} = \nabla \cdot (\nu + \nu_T / \sigma_k)\nabla \phi - \left(2\alpha\frac{\varepsilon}{k} + \frac{2\nu(\nabla\phi^{1/2} \cdot \nabla\phi^{1/2})}{\phi} + \frac{\varepsilon}{k}\frac{2}{(1 + C_{p3}\frac{\nu_T}{\nu})} \right)\phi$$
$$+ C_{p1}\frac{\varepsilon}{k}\frac{(1-\alpha)}{(1+25/Re)}(\tfrac{2}{3}k - \phi) + C_{p2}\frac{\phi}{k}P + (C_{p2} + C_{p4})2\alpha\frac{\phi}{k}\left(\frac{\psi \cdot \psi}{\nu_T(1+25/Re)} - P \right)$$

$$\frac{D\psi}{Dt} = \nabla \cdot (\nu + \nu_T / \sigma_k)\nabla \psi - \left(\alpha\frac{\varepsilon}{k} + \frac{2\nu(\nabla k^{1/2} \cdot \nabla\phi^{1/2})}{(k\phi)^{1/2}} + \frac{\varepsilon}{k}\frac{1}{(1 + C_{p3}\frac{\nu_T}{\nu})} \right)\psi$$
$$+ (1 - C_{p2})\phi\omega - C_{p1}\frac{\varepsilon}{k}\frac{(1-\alpha)}{(1+25/Re)}\psi + C_{p2}\frac{\psi}{k}P + (C_{p2} + C_{p4})2\alpha\frac{\psi}{k}\left(\frac{\psi \cdot \psi}{\nu_T(1+25/Re)} - P \right)$$

$$\nabla \cdot \mathbf{R} = \nabla\phi + \nabla \times \boldsymbol{\psi}$$

where

$$P = \psi \cdot \omega, \quad \nu_T = C_\mu \frac{\phi k}{\varepsilon}, \quad \beta = \left(\tfrac{1 + CwT2 * rr \cdot rr / Re}{1 + CwtT1 / Re} \right)^{1/2}, \quad \alpha = 1/(1 + 1.5\tfrac{\phi}{k}), \quad \text{and} \quad Re = k^2/(\nu\varepsilon).$$

The constants are:

$$\sigma_k = 0.8, \sigma_\varepsilon = 1.2, C_{\varepsilon 1} = 1.5, C_{\varepsilon 2} = 1.83, C_{\varepsilon 3} = 0.17, C_{p1} = 4.2, C_{p2} = \tfrac{3}{5}, C_{p3} = .12, C_{p4} = \tfrac{6}{7}.$$

The two constants given by fractions are determined by matching Rapid Distortion Theory (RDT) in the case of strongly sheared turbulence. A detailed derivation of these equations is found in Reference [2].

Initially these equations appear daunting. In fact, they represent a fairly simple extension of the classic k-ε equation system, and are relatively simple compared to Reynolds stress transport equation models. The second source term in the potential equations (in parentheses) is a dissipation-like term. This term is a standard dissipation model with two near-wall/surface modifications, one for the dissipation and one for the near wall pressure correlation term. These modifications are active in the laminar sublayer and allow the model to obtain the correct asymptotic behavior in the sublayer. The source terms involving the constants C_{p1} and C_{p2} are pressure-strain redistribution terms. The slow pressure-strain is based on return-to-isotropy and the fast pressure-strain is based on isotropization of the production model. The constants are set to common values for these models. The effect of system rotation can be explicitly included in the model, (as with a Reynolds stress transport equation model) but is not necessary in this context.

While the model includes transport equations for k and ε it should be emphasized that the proposed model is a significant departure from standard two-equation models. k and ε are now auxiliary quantities that are only used to help model the source terms in the turbulent potential evolution equations. They are not used to determine the Reynolds stress tensor or the resulting mean flow. The elimination of the constitutive equation for the Reynolds stresses is an important departure that removes one of the weaker modeling assumptions. A k-ω implementation could easily be substituted for the current choice of k and ε. The dissipation rate was chosen because some of the test cases have this quantity available for comparison. If computational time is a serious issue, algebraic models for either or both of these variables can be used. In particular, for shear dominated flows, $k = \frac{3}{2}(\phi + E\psi \cdot \psi / \phi)$ and $\varepsilon = C_\mu P \frac{\phi k}{\psi \cdot \psi}$ are good approximations. The latter expression is equivalent to the linear eddy viscosity hypothesis (though used in a different context). Computations of turbulent channel flow with these algebraic expressions and $E = 1.1$ showed a reasonable agreement with the DNS data of Kim, Moin & Moser[12].

Some of the important theoretical properties of the model are summarized below:

- Correct decay of homogeneous isotropic turbulence.
- Correct behavior in the log layer.
- Correct behavior for homogeneous shear flows at early times or after the sudden introduction of mean shear along a streamline.
- Correct behavior for homogeneous shear flows at long times.
- Exact asymptotic behavior near walls.
- Exact asymptotic behavior at free surfaces.
- No ad hoc damping functions or functions of the wall normal distance (which is poorly defined in complex geometries).
- No ad hoc manipulation of the model constants for different flows.
- Explicit dependence on system rotation if it is present.
- Natural relaminarization, and precise control of turbulence growth during transition.
- Stability/Numerical robustness (for the flows tested to date).
- A complexity roughly twice that of two-equation models and half that of Reynolds stress transport equation models. Note that most modern two equation models (see Durbin[13] and also Craft et al.[14]) add one or two additional PDEs making this model directly comparable in complexity to 'enhanced' two equation models.
- Exact transport equations (albeit unclosed) from which to derive the model terms. When adding additional physical effects (compressibility, particle interactions, buoyancy, etc.) the exact equations give a concrete analytical expression from which to construct the model extensions.
- No algebraic constitutive relations relating the turbulence to the mean flow.

4. ADVERSE PRESSURE GRADIENT BOUNDARY LAYERS

Adverse pressure-gradient boundary layers represent a situation where the classic assumptions of turbulence modeling are not well approximated. In particular, the turbulence is not in equilibrium with the mean flow, and the eddy viscosity hypothesis is a poor approximation. Two equation models (even the more elegant models, such as Durbin's elliptic relaxation model) tend to have some problems predicting adverse pressure boundary layers. However, models which predict the shear stress directly (Johnson & King, Bradshaw, Ferriss & Atwell, and full Reynolds stress closures) generally show considerably more success with these types of flows. Since the potential model also directly predicts a quantity akin to the shear stress, it is expected to perform well in these situations.

A common adverse pressure-gradient flow for tests of turbulence models is the experiment of Samuel & Joubert[15]. The experimental and computed velocity profiles at two downstream locations (Samuel & Joubert's station 9 and station 12) are shown in Figure 1. Only the nondimensional profiles are available for this experiment.

A more difficult test of the model's ability to capture separating flows is given by the experiments of Schubauer & Spangenberg[16]. This experiment has a very strong adverse pressure-gradient which comes very close to causing separation. The data is dimensional, which means that the boundary layer growth must also be predicted correctly for this test case. Figure 2 shows velocity profiles for the initial condition and three downstream locations of this flow compared with the experiments. The poorer agreement at the last station, close to separation, is thought to be a result of the boundary layer approximation, not necessarily the model.

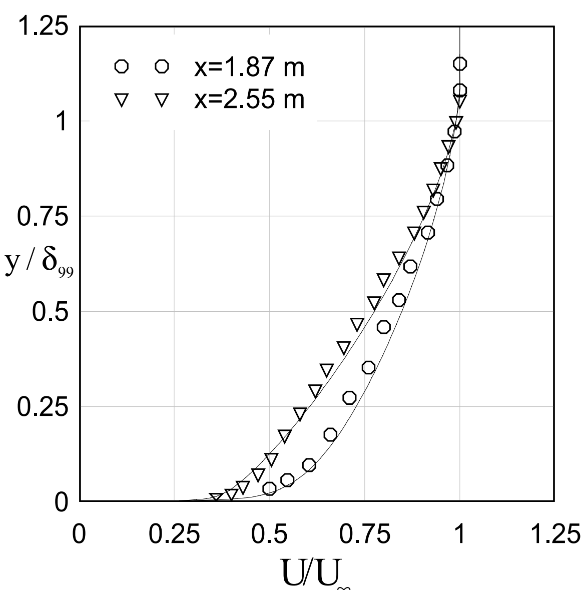

Figure 1*. Experimental (symbols) and calculated (lines) velocity for the Samuel & Joubert adverse pressure gradient boundary layer.*

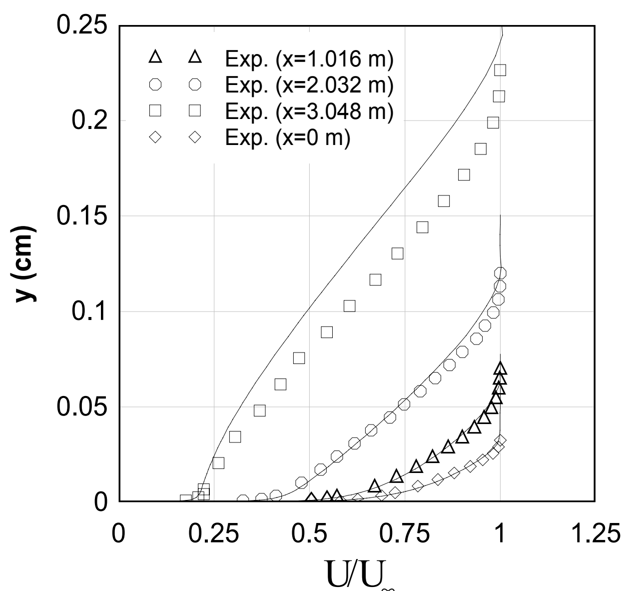

Figure 2*. Experimental (symbols) and calculated (lines) velocity profiles for the adverse pressure gradient boundary layer of Schubauer & Spangenberg.*

5. BACKWARD FACING STEP

The first backward facing step case is for a step with an expansion ratio of 1.2 and a Reynolds number of 5100 (based on the maximum velocity and step height, H). This geometry corresponds to the DNS simulations of Le & Moin[17] and the experimental results of Jovic & Driver[18]. The step is located at y/H=1 and x/H=0. The calculation domain extends from –3H upstream of the step to 27H downstream and 6H in the vertical direction. The mesh consisted of 120x120 quadrilateral cells stretched so as to resolve the boundary layers, shear layer, and the reattachment zone. The computed reattachment point was found to be 6.36 step-heights downstream of the step. This corresponds very favorably with the value of 6.28h found by the DNS simulations and 6.1h found by the experiments. DNS data and model predictions for the mean velocity are shown for a number of downstream positions in Figure 3. This figure focuses on a reduced area of the computational domain where the flow is most complex. Squares indicate the DNS results and solid lines indicate the model predictions. There appear to be some differences in the inlet velocity profile, and the magnitude of the velocity in the recirculation bubble is slightly underpredicted, but the overall agreement is reasonable.

The higher Reynolds number backstep experiment of Driver & Seegmiller[19] was also calculated. The Reynolds number is an order of magnitude larger (37,500) and the expansion ratio is somewhat smaller (1.125). The mesh was increased near the walls (to 140x140) to

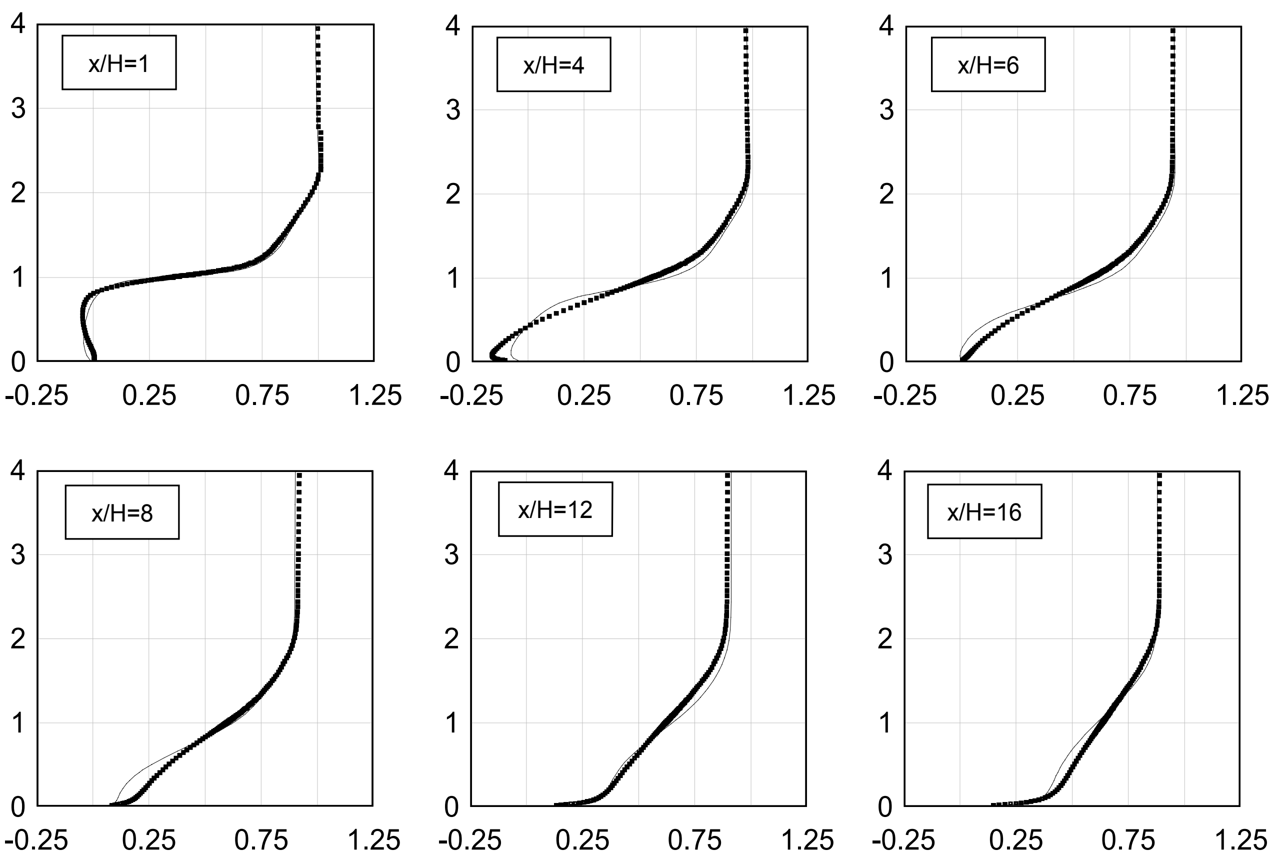

Figure 3. *Velocity profiles at several downstream positions for the low Re number backward facing step. Symbols, experimental data of Le & Moin. Solid lines, model predictions.*

capture the thinner boundary layers. Figure 4. shows the experimental and predicted velocity profiles at a number of downstream positions. The results are typical of low Reynolds number Reynolds stress transport equation models[20]. The reattachment point is well predicted but the strength of the recirculation zone is underpredicted, and the boundary layer does not recover quickly enough. It is believed that corrections to the vector potential equation could correct both of these deficiencies.

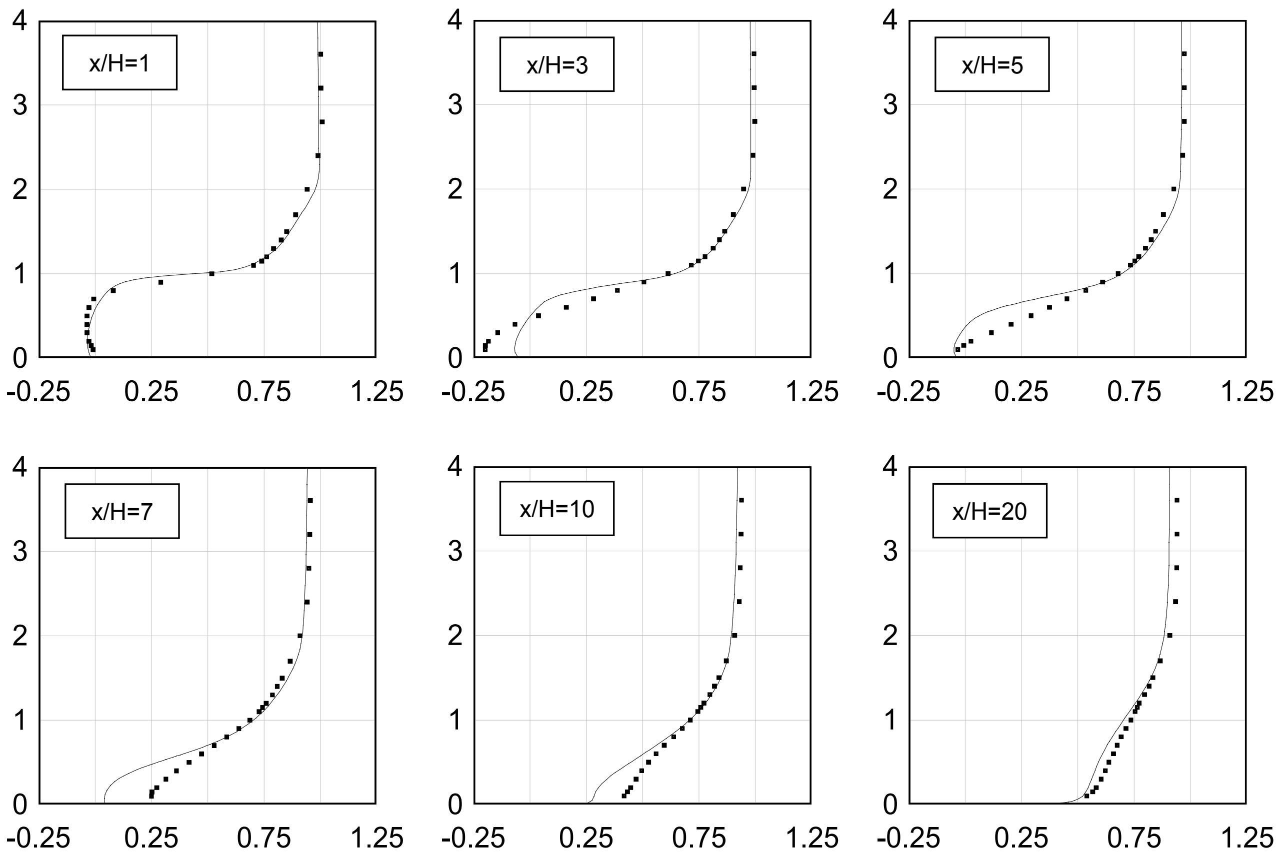

Figure 4. *Velocity profiles at several downstream positions for the high Re number backward facing step. Symbols, experimental data of Driver & Seegmiller. Solid lines, model predictions.*

6. IMPINGING JET

Calculations of an impinging slot jet were performed to test the accuracy of the model in stagnation point flows. Comparisons of the local Nusselt number on the base plate were made at a Reynolds numbers of 2900 (based on the jet width and average jet exit velocity) and a jet height of two nozzle widths (H/W=2). The local Nusselt number as a function of the distance from the jet centerline is shown in Figure 5. The peak value compares very well with the experimental data of Martin[21]. It is suspected that coarse mesh resolution towards the domain exit reduces the quality of the predictions far from the jet centerline. Standard two-equation models incorrectly predict the maximum Nusselt number by as much as 100%. This is due to the spurious production of kinetic energy on the portion of the plate directly beneath the jet (in the stagnation region). The success of the turbulent potential model is attributed to the fact that it does not produce kinetic energy in the stagnation region. Contours of the turbulent kinetic energy are displayed in Figure 6. to demonstrate this fact. Due to symmetry considerations only one half of the domain is displayed. The jet enters at the top left of the domain and exits to the right.

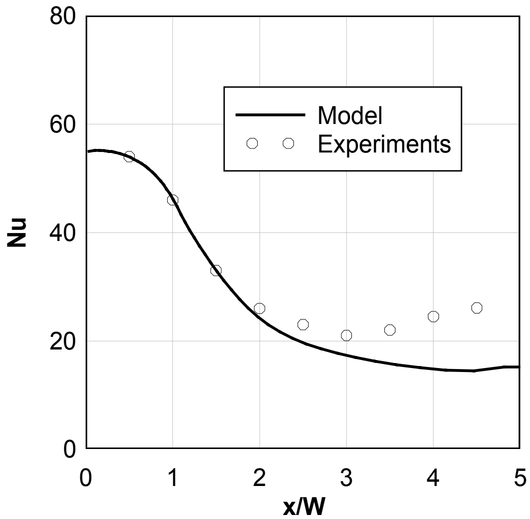

Figure 5. Local Nusselt number as a function of distance from the jet centerline. Re=2900.

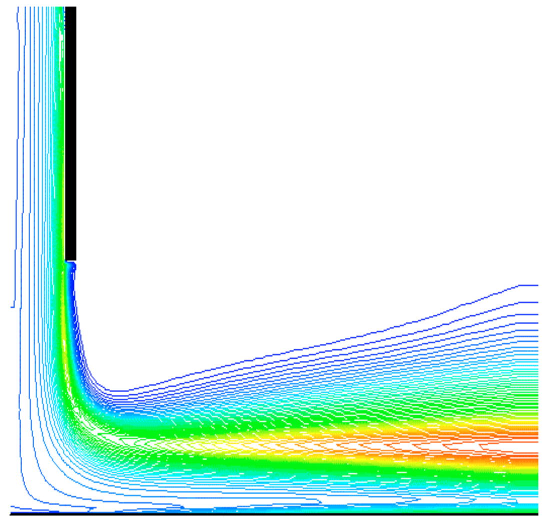

Figure 6. Contours of turbulent kinetic energy. Note the lack of kinetic energy at the stagnation point.

7. CONCLUSION

Calculations of relatively complex turbulent flows were performed using the turbulent potential model. The model produced predictions that were superior to many two-equation models and comparable to Reynolds stress transport equation models. However, we estimate the computational cost of the turbulent potential model to be very similar to enhanced two equation models. It was found that the transport equations for the potentials could be uncoupled and updated individually and that the system of equations was no stiffer than a standard k/ε implementation. The proposed transport equations can be integrated up to a wall or surface; they do not require wall functions. In addition, no *ad hoc* functions of the wall normal coordinate have been used, so the model can be implemented easily into existing flow solvers and complex geometries.

ACKNOWLEDGEMENTS

This work was funded, in part, by NASA-Ames Research Center in the form of a Phase I SBIR Grant. Their support is gratefully acknowledged.

REFERENCES

1. B. Perot & P. Moin, “A new approach to turbulence modeling”, Proc. of the 1996 Summer Program, Center for Turbulence Research, Stanford University/NASA Ames, 35-46 (1996).
2. B. Perot, “Turbulence modeling using body force potentials”, Submitted to Phys. Fluids, Sept. (1998).
3. W. Rodi, “A new algebraic relation for calculating the Reynolds stresses”, ZAMM **56**, 219-221 (1976).
4. S. B. Pope, “A more general effective-viscosity hypothesis”, J. Fluid Mech. **72**, 331-340 (1975).
5. T. B. Gatski & C. G. Speziale, “On explicit algebraic stress models for complex turbulent flows”, J. Fluid Mech. **254**, 59-78 (1993).
6. D. A. Johnson & L. S. King, “A mathematically simple turbulence closure model for attached and separated turbulent boundary layers”, AIAA Journal, **23** (11), 1684-1692 (1985)
7. P. Bradshaw, D. H. Ferriss & N. P. Atwell, “Calculations of boundary-layer development using the turbulent energy equation”, J. Fluid Mech. **28**, 593-616 (1967).
8. S. J. Kline, M. V. Cockrell, M. V. Morkovin & G. Sovan, eds. *Computation of Turbulent Boundary-Layers*, *Vol I*, AFOSR-IFP-Stanford Conference. (1968).
9. U. Schumann, “Realizability of Reynolds-stress models”, Phys. Fluids **2**0, 721-725 (1977).
10. J. Wu, Y. Zhou & J. Wu, “Reduced stress tensor and dissipation and the transport of the Lamb vector”, ICASE Report No 96-2, (1996)
11. H. Marmanis, “Analogy between the Navier-Stokes equations and Maxwell’s equations: applications to turbulence”, Phys. Fluids **10** (6), 1428-1437 (1998)
12. J. Kim, P. Moin & R. Moser, “Turbulence statistics in fully developed channel flow at low Reynolds number”, J. Fluid Mech. **177**, 133-166 (1987).
13. P. A. Durbin, “A Reynolds stress model for near-wall turbulence”, J. Fluid Mech. **249**, 465-498 (1993).
14. T. J. Craft, B. E. Launder & K Suga,. “A non-linear eddy-viscosity model including sensitivity to stress anisotropy”, Proc. 10th Symp. Turbulent Shear Flows, Pennsylvania State University, (1995).
15. A. E. Samuel & P. N. Joubert, “A boundary layer developing in an increasingly adverse pressure gradient”, J. Fluid Mech. **66**, 481-505 (1974).
16. G. B. Schubauer & W. G. Spangenberg, “Flow A”*, Computation of Turbulent Boundary Layers, Volume II – Compiled Data*., D. E. Coles & E. A. Hirst, eds., 416 (1968).
17. H. Le, P. Moin & J. Kim, “Direct numerical simulation of turbulent flow over a backward-facing step”, J. Fluid Mech. **330**, 349-374 (1997).
18. S. Jovic & D. M. Driver, “Reynolds number effects on the skin friction in separated flows behind a backward facing step”. Experiments in Fluids **18**, 464-467 (1995).
19. D. Driver & H. L. Seegmiller, “Features of reattaching turbulent shear layer in divergent channel flow”, AIAA J., **23**, 162-171 (1985).
20. S. H. Ko, “Computation of turbulent flows over backward and forward-facing steps using a near-wall Reynolds stress model”, CTR Annual Research Briefs, Stanford University/NASA Ames, 75-90 (1993).
21. H. Martin, “Heat and mass transfer between gas jets and solid surfaces”, Adv. Heat Trans., **13**, 1-59 (1977).